CrossMark

ORIGINAL ARTICLE

Diagnostic accuracy of ^{18}F-FDG PET/CT compared with that of contrast-enhanced MRI of the breast at 3 T

Heinrich F. Magometschnigg[1] · Pascal A. Baltzer[1] · Barbara Fueger[1] ·
Thomas H. Helbich[1] · Georgios Karanikas[2] · Peter Dubsky[3] · Margaretha Rudas[4] ·
Michael Weber[1] · Katja Pinker[1,5]

Abstract

Purpose To compare the diagnostic accuracy of prone ^{18}F-FDG PET/CT with that of contrast-enhanced MRI (CE-MRI) at 3 T in suspicious breast lesions. To evaluate the influence of tumour size on diagnostic accuracy and the use of maximum standardized uptake value (SUV$_{MAX}$) thresholds to differentiate malignant from benign breast lesions.

Methods A total of 172 consecutive patients with an imaging abnormality were included in this IRB-approved prospective study. All patients underwent ^{18}F-FDG PET/CT and CE-MRI of the breast at 3 T in the prone position. Two reader teams independently evaluated the likelihood of malignancy as determined by ^{18}F-FDG PET/CT and CE-MRI independently. ^{18}F-FDG PET/CT data were qualitatively evaluated by visual interpretation. Quantitative assessment was performed by calculation of SUV$_{MAX}$. Sensitivity, specificity, diagnostic accuracy, area under the curve and interreader agreement were calculated for all lesions and for lesions <10 mm. Histopathology was used as the standard of reference.

Results There were 132 malignant and 40 benign lesions; 23 lesions (13.4 %) were <10 mm. Both ^{18}F-FDG PET/CT and CE-MRI achieved an overall diagnostic accuracy of 93 %. There were no significant differences in sensitivity ($p=$ 0.125), specificity ($p=0.344$) or diagnostic accuracy ($p=1$). For lesions <10 mm, diagnostic accuracy deteriorated to 91 % with both ^{18}F-FDG PET/CT and CE-MRI. Although no significant difference was found for lesions <10 mm, CE-MRI at 3 T seemed to be more sensitive but less specific than ^{18}F-FDG PET/CT. Interreader agreement was excellent ($\kappa=$ 0.85 and $\kappa=0.92$). SUV$_{MAX}$ threshold was not helpful in differentiating benign from malignant lesions.

Conclusion ^{18}F-FDG PET/CT and CE-MRI at 3 T showed equal diagnostic accuracies in breast cancer diagnosis. For lesions <10 mm, diagnostic accuracy deteriorated, but was equal for ^{18}F-FDG PET/CT and CE-MRI at 3 T. For lesions <10 mm, CE-MRI at 3 T seemed to be more sensitive but less specific than ^{18}F-FDG PET/CT. Quantitative assessment using an SUV$_{MAX}$ threshold for differentiating benign from malignant lesions was not helpful in breast cancer diagnosis.

✉ Thomas H. Helbich
thomas.helbich@meduniwien.ac.at

1 Department of Biomedical Imaging and Image-guided Therapy, Division of Molecular and Gender Imaging, Medical University of Vienna, Vienna, Austria

2 Department of Biomedical Imaging and Image-guided Therapy, Division of Nuclear Medicine, Medical University of Vienna, Vienna, Austria

3 Department of Surgery, Medical University of Vienna, Vienna, Austria

4 Department of Pathology, Medical University of Vienna, Vienna, Austria

5 Molecular Imaging and Therapy Service, Memorial Sloan Kettering Cancer Center, New York, USA

Introduction

Contrast-enhanced MRI (CE-MRI) is a well-established imaging modality for the detection, characterization and staging of breast tumours [1]. The sensitivity of CE-MRI for the depiction of breast carcinoma has been reported to be in the range of 89 – 100 %. Although CE-MRI is extremely sensitive, specificity is limited, ranging from 67 % to 80 %, which leads to additional work-up and biopsies of benign lesions [1]. Several studies have investigated the use of higher magnet

field strengths (3 T) and high-resolution CE-MRI protocols, which allow a more detailed depiction of lesion morphology and enhancement kinetics, and have demonstrated an improvement in diagnostic accuracy [2–6].

Recently, ^{18}F-FDG PET/CT has emerged as a valuable tool in breast imaging, particularly when examinations are performed in the prone position [7–10]. ^{18}F-FDG PET/CT has been shown to be a valuable technique, with sensitivities ranging from 80 % to 87 % and specificities ranging from 73 % to 100 % [10, 11]. Furthermore, it seems that prone ^{18}F-FDG PET/CT is more specific than CE-MRI. However, a direct comparison with state-of-the-art CE-MRI at 3 T has not yet been performed. If ^{18}F-FDG PET/CT achieves results comparable to those with CE-MRI at 3 T, it could then be used as a substitute in those patients who are not candidates for MRI [12] and vice versa.

We hypothesized that ^{18}F-FDG PET/CT could achieve results that are at least comparable to those with CE-MRI at 3 T. The aim of this study was threefold:

1. To compare the diagnostic accuracy of prone ^{18}F-FDG PET/CT with that of CE-MRI at 3 T in breast lesions
2. To evaluate whether the diagnostic accuracy is influenced by lesion size
3. To determine whether quantitative assessment of PET data using maximum standardized uptake values (SUV_{MAX}) is helpful in the characterization of malignant and benign breast lesions, compared to qualitative visual assessment.

Materials and methods

Patients

Of 198 consecutive patients, 172 (age range 18 – 87 years, mean 57 years) who fulfilled the following inclusion criteria were enrolled from September 2009 to May 2013 in this prospective, institutional review board-approved study: age >18 years, suspicious findings on mammography or breast ultrasonography (BI-RADS® category 0, 4 and 5), not pregnant or breastfeeding, no previous treatment (e.g. breast biopsy, neoadjuvant chemotherapy), and no contraindications to MRI or MRI contrast agents. The remaining 28 patients were excluded because of incomplete examinations or prior treatment. Written informed consent was obtained from all patients before the examinations. Regardless of the results of either prone ^{18}F-FDG PET/CT or CE-MRI at 3 T, histopathological verification of all suspicious lesions was performed and was used as the gold standard. The initial BI-RADS® categories of lesions before the study examinations were: 0 for 18 lesions, 4 for 63 lesions, and 5 for 91 lesions.

Imaging

All patients underwent prone ^{18}F-FDG PET/CT and CE-MRI of the breast at 3 T. Examinations were scheduled no longer than 7 days apart (same day in 60 patients, 1 day in 28, 2 days in 13, 3 days in 8, 4 days in 11, 5 days in 7, 6 days in 4, 7 days in 41; range 0 – 7 days, mean 3 days).

^{18}F-FDG PET/CT

Prone ^{18}F-FDG PET/CT of the breast was performed using a combined whole-body PET/CT in-line system (Biograph 64 TruePoint®; Siemens, Erlangen, Germany) equipped with a high-resolution PET scanner and a 64-row detector CT scanner. Patients were required to fast for at least 5 h before injection of approximately 200 – 350 MBq ^{18}F-FDG based on body weight and to have a blood glucose level <150 mg/dl (8.3 mmol/l). Scanning was started 60 min after intravenous injection of ^{18}F-FDG as a bolus. Initially, a prone low-dose CT scan without contrast agent from the base of the skull to the upper abdominal region was acquired for attenuation correction. To enable the same patient geometry as with CE-MRI a commercially available cushion (GE Healthcare) for supporting a patient in a prone position during the PET scan was used. Subsequently, a high-resolution prone PET dataset over the same region was recorded. PET images were reconstructed using the iterative TrueX algorithm (Siemens, Erlangen, Germany). This algorithm incorporates a particular correction for the point-spread function in addition to usually used correction factors [13, 14]. Four iterations per 21 subsets were used with a matrix size of 168×168, a transaxial FOV of 605 mm (pixel size 3.6 mm) and a section thickness of 5 mm.

CE-MRI

All patients were examined with a 3 T MRI scanner (Tim Trio®; Siemens, Erlangen, Germany) in the prone position using a dedicated, four-channel breast coil (InVivo®; Orlando, FL). In premenopausal women, the MRI examination was performed during the second week of the menstrual cycle to reduce breast parenchymal background enhancement [1]. A T2-weighted turbo inversion recovery magnitude (TIRM) sequence with fat suppression was used (TR/TE 4,800/59 ms, FOV 340 mm, 48 slices at SI 3 mm, flip angle 120°, matrix 384×512, acquisition time 2 min 35 s) together with a split dynamics, contrast-enhanced MRI protocol [4] with the following parameters: T1-weighted volume-interpolated breathhold examination (VIBE) sequences (TR/TE 3.61/1.4 ms, FOV 320 mm, 72 slices, 1.7 mm isotropic, matrix 192×192, one average, 13.2 s per volume), and T1-weighted turbo fast-low-angle shot (FLASH) 3D sequences with selective water excitation (TR/TE 877/3.82 ms, FOV 320 mm, 96 slices, 1 mm isotropic, matrix 320×134, one average, 2 min). The total acquisition time was approximately 15 min 20 s.

The contrast agent used was gadoterate meglumine (Dotarem®; Guerbet, France), which was administered intravenously as a bolus (0.1 mmol/kg body weight) using a power injector (Spectris Solaris EP®; Medrad, Pittsburgh, PA).

Data analysis

Two experienced nuclear medicine specialists (reader 1 with 7 years experience, reader 2 with 15 years experience) assessed the ^{18}F-FDG PET/CT data independently. Two experienced breast radiologists (reader 3 with 7 years experience, reader 4 with 11 years experience) evaluated the CE-MRI data independently. The readers were aware of the inclusion criteria, but were not provided with clinical histories or previous imaging findings. Lesions were assessed on a patient-by-patient basis. In patients with multiple lesions, the readers were asked to assess the most suspicious lesion. Lesion locations were recorded clockwise in quadrants. After data analysis, the recorded lesion locations were compared to identify potential lesion mismatches.

^{18}F-FDG PET/CT

Two readers qualitatively evaluated all prone ^{18}F-FDG PET/CT images visually for increased tracer uptake by breast lesions. Lesions with focal uptake above background activity were classified as malignant. If no focal ^{18}F-FDG uptake was apparent, ^{18}F-FDG PET/CT was considered negative for malignancy. Fatty and normal fibroglandular tissue within the breast served as background tissue. If there was disagreement between the readers, a consensus decision was reached and used for statistical analysis. SUV_{MAX} was calculated, but no threshold for malignancy was applied [15, 16]. To measure SUV_{MAX}, a region of interest was drawn over the area of focal ^{18}F-FDG uptake by both readers. If no focal ^{18}F-FDG uptake was apparent, the lesion was localized with CE-MRI and a corresponding region of interest was placed on the PET images.

CE-MRI

Lesions were classified as masses or non-mass-enhancing (NME) lesions. Criteria for distinguishing benign from malignant contrast-enhancing lesions were based on the morphology and enhancement kinetics defined by the revised American College of Radiology (ACR) BI-RADS® atlas [17]. The probability of malignancy was determined by assigning a final BI-RADS® assessment category [17]. If findings were discordant between readers, a consensus decision was reached and used for statistical analysis. For the assessment of the enhancement characteristics of masses, an automated, semiquantitative, curve-type analysis was performed using dedicated software (Syngo BreVis; Siemens, Erlangen, Germany). For NME lesions, kinetics were not considered [18, 19]. The size of the index lesion was assessed using the largest diameter in the axial plane on CE-MRI.

Histopathology

The histopathological result was considered the final diagnosis in all patients. Using image-guided needle biopsy, surgical biopsy, mastectomy or lumpectomy, the histopathological diagnosis was established by one pathologist (M.R., with >20 years experience). If both the image-guided needle biopsy and imaging findings were benign, the final diagnosis was considered benign (33 patients). If the findings were discordant between image-guided needle biopsy and imaging, the final diagnosis was established by surgery (7 patients). If a lesion was high risk or had an uncertain potential for malignancy on image-guided needle biopsy, the final diagnosis was established by surgery (7 patients) [20]. All patients with malignant lesions underwent surgery after image-guided needle biopsy (132 patients).

Statistical methods

Prior to data analysis, the recorded lesion locations were compared for potential lesion mismatch, and no mismatches were found. Statistical tests were performed by a statistician (M.W., 14 years of experience) using SPSS 19.0 and CIA version 2.2.0. For statistical analysis, the assigned BI-RADS® assessment categories for CE-MRI data were dichotomized. BI-RADS® 2 and 3 were considered benign, and 4 and 5 malignant. Sensitivity, specificity, diagnostic accuracy, positive predictive value and negative predictive value for ^{18}F-FDG PET/ CT and CE-MRI were calculated. Differences in sensitivity, specificity and diagnostic accuracy were assessed by McNemar and Cochran Q tests. Receiver operating characteristic (ROC) curves were calculated, the area under the curve was determined, and the significance of differences was assessed using the DeLong method. SUV_{MAX} was evaluated for its potential to differentiate benign from malignant lesions

Table 1 Histopathological results of all breast lesions

Histology	No. (%) of lesions	Size (mm), mean (range)
Malignant	132 (76.7)	
Ductal carcinoma in situ	8 (4.7)	22.75 (3 – 89)
Invasive ductal carcinoma	106 (61.6)	28.2 (5 – 97)
Invasive lobular carcinoma	13 (7.6)	30.69 (12 – 57)
Mucinous carcinoma	3 (1.7)	19.4 (15 – 28)
Micropapillary carcinoma	1 (0.6)	24
Melanoma metastasis	1 (0.6)	25
Benign	40 (23.3)	
Fibroadenoma/ fibroadenomatous hyperplasia	17 (9.9)	20 (6 – 50)
Miscellaneous	16 (9.3)	19.19 (5 – 67)
B3 lesions	7 (4.1)	21.71 (7 – 50)

Table 2 Sensitivity, specificity, positive predictive value, negative predictive value, diagnostic accuracy and area under the curve of ^{18}F-FDG PET/CT and CE-MRI together with p values and 95 % confidence intervals (in parentheses) for all 172 lesions

	Sensitivity (%)	Specificity (%)	Positive predictive value (%)	Negative predictive value (%)	Accuracy (%)	Area under the curve
^{18}F-FDG PET/CT	97 (0.93 – 0.99)	80 (0.65 – 0.9)	94.1 (0.89 – 0.97)	88.9 (0.75 – 0.96)	93 (0.88 – 0.96)	0.89 (0.73 – 0.91)
CE-MRI	100 (0.97 – 1)	70 (0.55 – 0.82)	91.7 (0.86 – 0.95)	100 (0.88 – 1)	93 (0.88 – 0.96)	0.85 (0.76 – 0.94)
p value	0.125	0.344	NA	NA	1	NA

*p<0.05

using ROC analysis and Welch-corrected t tests. Interreader variability for diagnosis with ^{18}F-FDG PET/CT and CE-MRI was assessed using κ-statistics. A p value ≤0.05 was considered significant.

Results

The mean size of the 172 breast tumours was 26.02 mm (range 5 – 97 mm). Of these 172 lesions, 40 (23 %) were benign and 132 (77 %) were malignant. Twenty three lesions (13 %) were <10 mm, of which 9 were malignant and 14 were benign. Histopathological diagnoses are summarized in Table 1.

The diagnostic values for ^{18}F-FDG PET/CT and CE-MRI at 3 T for all lesions are summarized in Table 2, and for lesions <10 mm in Table 3. There were no significant differences in sensitivity, specificity or diagnostic accuracy between ^{18}F-FDG PET/CT and CE-MRI at 3 T for all lesions (Fig. 1, Table 2) or for lesions <10 mm (Table 3).

^{18}F-FDG PET/CT classified 136 lesions as malignant (Fig. 2) and 36 lesions as benign (Figs. 3 and 4). Diagnostic accuracy was influenced by lesion size and decreased from 93 % to 91 % in lesions <10 mm. There was excellent interreader agreement for ^{18}F-FDG PET/CT (κ=0.85).

On ^{18}F-FDG PET/CT, SUV$_{MAX}$ ranged from 1.03 to 6.52 in benign lesions (mean SUV$_{MAX}$ 2.49, SD 1.13) and from 1.1 to 36.02 in malignant lesions (mean SUV$_{MAX}$ 6.11, SD 5.9). There was a significant difference in SUV$_{MAX}$ between malignant and benign tumours (p<0.001; Fig. 5). However, quantitative assessment using an SUV$_{MAX}$ threshold was not helpful for differentiating benign from malignant breast

tumours (Table 4). With ^{18}F-FDG PET/CT, there were eight false-positives (FP) and four false-negatives (FN) (Table 5).

On CE-MRI, there were 152 enhancing masses (mean size 24.7 mm, range 5 – 94 mm) and 20 NME lesions (mean size 35.9 mm, range 3 – 97 mm). CE-MRI classified 144 lesions as malignant (Figs. 2, 3, and 4) and 28 lesions as benign.

Of 30 benign mass lesions, 14 (47 %) showed a type 1 curve, 13 (43 %) a type 2 curve, and 3 (10 %) a type 3 curve. Of 122 malignant mass lesions, 5 (4 %) showed a type 1 curve, 42 (34 %) a type 2 curve, and 75 (62 %) a type 3 curve. There was excellent inter-reader agreement for CE-MRI at 3 T (κ=0.92). With CE-MRI there were 12 FP (Fig. 4) and no FN (Table 5).

Discussion

Our results indicate that both ^{18}F-FDG PET/CT and CE-MRI at 3 T provide equally high diagnostic accuracy with excellent interreader agreement. Although the results were influenced by lesion size, there were no significant differences in diagnostic accuracy between ^{18}F-FDG PET/CT and CE-MRI. Our results demonstrate that quantitative assessment of ^{18}F-FDG PET/CT using SUV$_{MAX}$ was not helpful in differentiating benign from malignant lesions. To date, few studies have investigated the ability of ^{18}F-FDG PET or ^{18}F-FDG PET/CT to differentiate malignant from benign breast lesions, and have shown lower diagnostic accuracies. The divergent results compared to this study may be explained by differences in study design and hardware, such as patient positioning (prone vs. supine), qualitative visual versus quantitative

Table 3 Sensitivity, specificity, positive predictive value, negative predictive value, diagnostic accuracy and area under the curve of ^{18}F-FDG PET/CT and CE-MRI together with p values and 95 % confidence intervals (in parentheses) for 23 lesions <10 mm

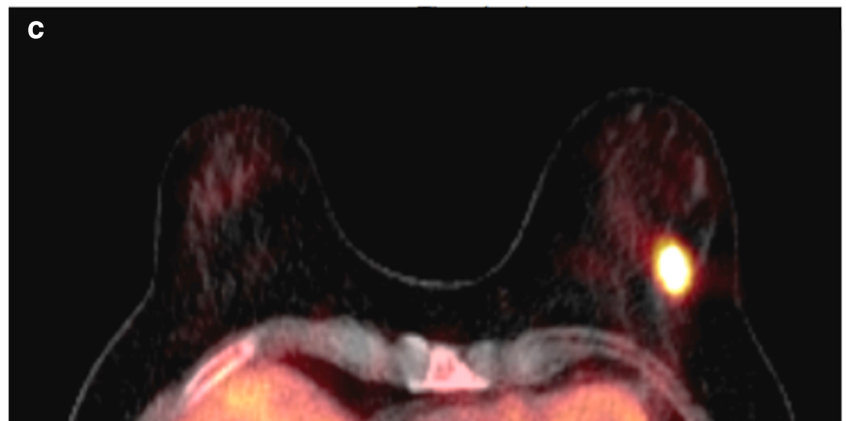|	Sensitivity (%)	Specificity (%)	Positive predictive value (%)	Negative predictive value (%)	Accuracy (%)	AUC
^{18}F-FDG PET/CT	78 (0.45 – 0.94)	100 (0.79 – 1)	100 (0.65 – 1)	88 (0.64 – 0.97)	91 (0.73 – 0.98)	0.89 (0.72 – 1)
CE-MRI	100 (0.66 – 100)	86 (0.57 – 0.98)	82 (0.48 – 0.97)	100 (0.73 – 1)	91 (0.73 – 0.98)	0.93 (81.4 – 1)
p value	0.5	0.5	NA	NA	1	NA

*p<0.05
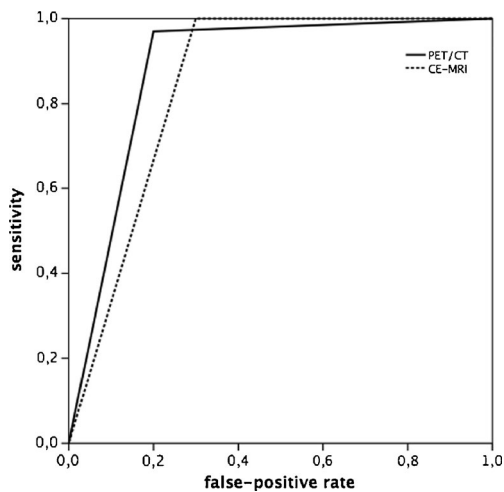
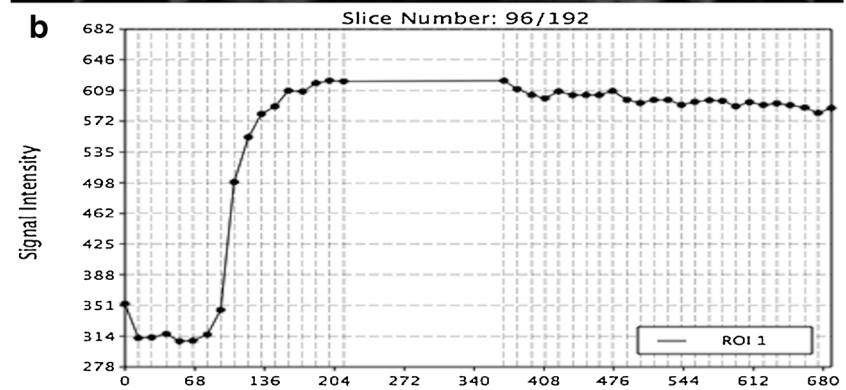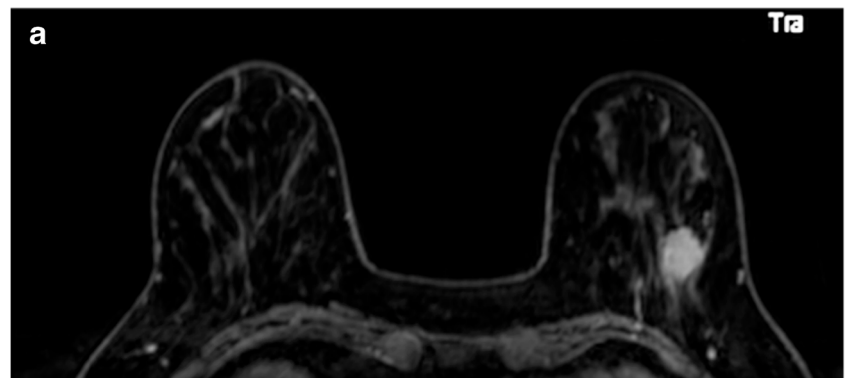**Fig. 1** ROC analysis shows that the diagnostic value of ^{18}F-FDG PET/CT is not significantly different from that of CE-MRI at 3 T

interpretation of data, and the use of different equipment (PET vs. PET/CT vs. dedicated breast PET scanners) [11, 21–23]. Adequate patient positioning is of importance for any imaging examination. It has been demonstrated that prone rather than supine patient position during ^{18}F-FDG PET or ^{18}F-FDG PET/CT examination improves breast cancer detection due to better delineation of lesions by expansion of the breast parenchyma, as well as higher influx of ^{18}F-FDG to the breast [7–9, 24, 25]. Previous studies have investigated ^{18}F-FDG PET and ^{18}F-FDG PET/CT in breast cancer patients and shown lower sensitivities (approximately 90 %) using supine patient positioning [26, 27]. In this study, we used prone patient positioning and a state-of-the-art combined PET/CT scanner, which explains the higher sensitivity and diagnostic accuracy achieved.

Fig. 2 Invasive ductal carcinoma (high-grade) laterally in the left breast in a 40-year-old woman. **a, b** The round, irregularly marginated mass lesion (**a**) shows a heterogeneous initial strong enhancement followed by a washout phase (**b**), and was classified by CE-MRI as BI-RADS® 5 (suspicious). **c** On the ^{18}F-FDG PET/CT image, the lesion is strongly ^{18}F-FDG-avid, with an SUV$_{MAX}$ of 16.83. The lesion was true-positive by both modalities

Fig. 3 Invasive lobular carcinoma (intermediate grade) laterally in the left breast in a 53-year-old woman. **a, b** The irregularly shaped and marginated mass lesion (**a**) shows a heterogeneous medium initial enhancement followed by a plateau (**b**), and was classified by CE-MRI as BI-RADS® 4 (suspicious). **c** On the ^{18}F-FDG PET/CT image, the mass is not significantly ^{18}F-FDG-avid, with an SUV_{MAX} of 1.9. The lesion was a true-positive finding by DCE-MRI at 3 T and false-negative by ^{18}F-FDG PET/CT
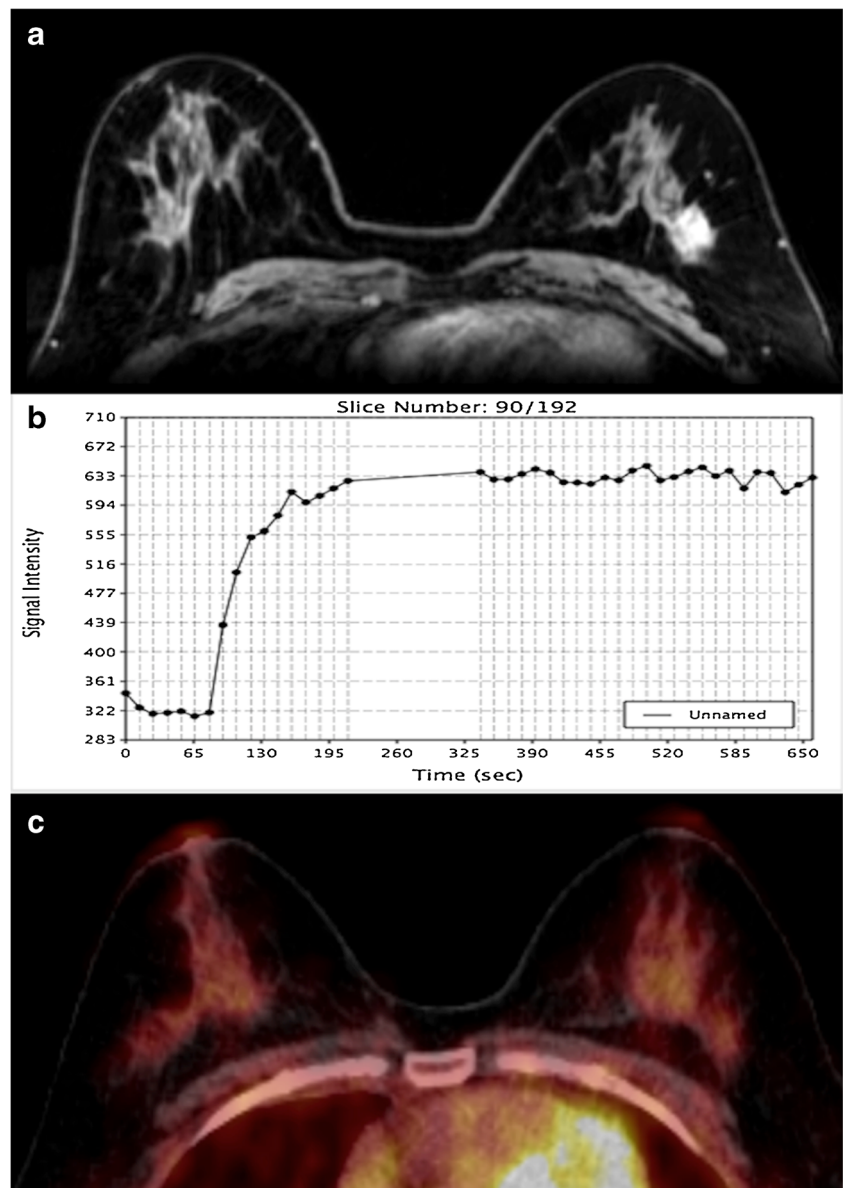
The approach to the interpretation of imaging data also influences diagnostic accuracy. Studies have investigated the quantitative assessment of ^{18}F-FDG PET/CT data using SUV_{MAX} thresholds in breast cancer diagnosis and have shown lower diagnostic accuracies of about 85 % [22, 23]. The results of our study confirm that quantitative data interpretation using an SUV_{MAX} threshold does not help in differentiating benign from malignant tumours, compared to qualitative visual assessment and thus should be omitted. The qualitative visual assessment approach yielded diagnostic accuracies of 93 % for all lesions and 91 % for lesions <10 mm. Thus, the data support the notion that ^{18}F-FDG PET/CT is a valuable tool in detecting breast cancer in patients with BI-RADS® 4, 5 or 0 lesions.

In this study, we employed the above-mentioned strategies and used state-of the art equipment, which contributed to the excellent results of ^{18}F-FDG PET/CT of the breast. However, due to the limited spatial resolution of ^{18}F-FDG PET/CT, its diagnostic value was lower in lesions <10 mm [10, 11, 22, 27]. Whereas with CE-MRI the excellent sensitivity of 100 % was sustained in lesions <10 mm, the sensitivity of ^{18}F-FDG PET/CT was reduced to 78 %, indicating that smaller lesions may be missed when not highly metabolically active. However, due to excellent specificity, the diagnostic accuracies of ^{18}F-FDG PET/CT and CE-MRI were equal in lesions <10 mm.

^{18}F-FDG PET/CT seems to be as useful as CE-MRI at 3 T for the assessment of breast tumours, but has some disadvantages, which limit its overall application in breast imaging. One inherent limitation is the whole-body radiation exposure [28]. Nevertheless, in patients with a suspicious finding, the modest radiation exposure seems justified. Due to the

Fig. 4 A high-risk retroareolar lesion (atypical ductal hyperplasia) medially in the right breast in a 32-year-old woman. **a**, **b** The irregularly shaped and spiculated mass lesion (**a**) shows persistent enhancement (**b**), and was classified by CE-MRI as BI-RADS® 4 (suspicious). **c** On the ^{18}F-FDG PET/CT image, the mass is not significantly ^{18}F-FDG-avid, with an SUV_{MAX} of 2.8. The lesion was true-negative by ^{18}F-FDG PET/CT and false-positive by CE-MRI at 3 T
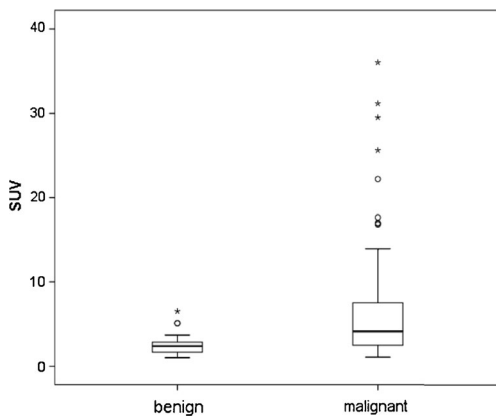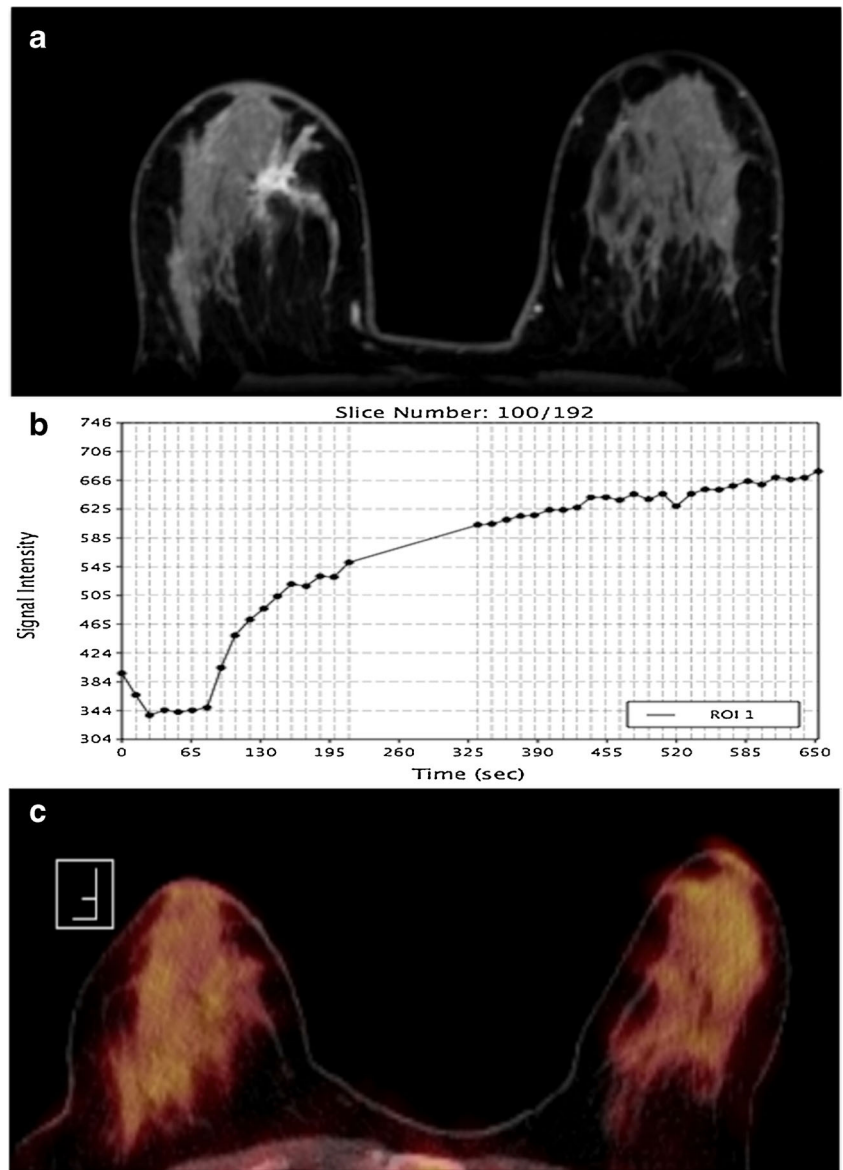

Fig. 5 Distribution of SUV_{MAX} values for benign and malignant breast lesions. Quantitative assessment using an SUV_{MAX} threshold was not helpful for differentiating benign from malignant breast tumours

Table 4 Sensitivity and false-positive rate of SUV_{MAX} thresholds for differentiating benign from malignant breast tumours using ^{18}F-FDG PET/CT

SUV_{MAX} threshold	Sensitivity (%)	False-positive rate (%)
1.06	100	97.5
1.9	89.4	65
2.3	78.8	52.5
2.5	75	42.5
2.8	67.4	27.5
3.0	62.1	20
3.5	57.6	12.5
4.0	52.3	7.5

Table 5 False-positive and false-negative lesions on ^{18}F-FDG PET/CT and contrast-enhanced MRI at 3 T on the basis of histopathological diagnosis

False-positive				False-negative[a]	
^{18}F-FDG PET/CT		CE-MRI		^{18}F-FDG PET/CT	
Finding	No. of lesions	Finding	No. of lesions	Finding	No. of lesions
Fibroadenoma/fibroadenomatous hyperplasia	5	Fibroadenoma/fibroadenomatous hyperplasia	3	Grade 1 invasive ductal carcinoma	1
High-risk (atypical ductal hyperplasia)	1	High-risk (atypical ductal hyperplasia, fibroadenomatous hyperplasia with atypia)	3	Grade 2 invasive ductal carcinoma	1
Mastitis	1	Ductal hyperplasia	1	Grade 3 invasive ductal carcinoma	1
Scar	1	Gynecomastia	1	Grade 2 invasive lobular carcinoma	1
Total	8	Mastitis	1	Total	4
		Scar	1		
		Adenosis	1		
		Pseudoangiomatous stromal hyperplasia	1		
		Total	12		

[a] There were no false-negative findings on CE-MRI

necessary delay of at least 45 min after tracer administration [29], ^{18}F-FDG PET/CT is more time-consuming than MRI of the breast by approximately 20 min [4]. The imaging accuracy of ^{18}F-FDG PET/CT is affected by tumour histology. Diffuse or slowly growing cancers, such as lobular carcinoma, or low-grade ductal carcinoma in situ (DCIS), can be missed with ^{18}F-FDG PET/CT [10], but this also applies to CE-MRI, and the performance of the two modalities in these lesions seems to be equal. In addition, it has been demonstrated that the performance of ^{18}F-FDG PET/CT in these subtypes can be improved by dual time-point acquisition [27]. An advantage of ^{18}F-FDG PET/CT is that, in patients with a high level of suspicion for breast malignancy, lymph node, or even distant metastases, an additional supine whole-body ^{18}F-FDG PET/CT scan for staging can be performed in a single session. It has been demonstrated that such a combined prone and supine whole-body ^{18}F-FDG PET/CT scan may influence further therapeutic decisions by detecting a greater number of distant metastases than conventional staging algorithms [24]. The radiotracer used in the current study was ^{18}F-FDG. It has been demonstrated that ^{18}F-FDG has good sensitivity but limited specificity, as several types of benign breast diseases can be [18]FDG-avid and mimic malignancy [10]. In this study the majority of FP findings were metabolically active fibroadenomas/fibroadenomatous hyperplasia together with a high-risk lesion (atypical ductal hyperplasia), mastitis and a scar.

CE-MRI of the breast is an established imaging modality routinely used for the assessment of breast tumours, with reported excellent sensitivities (98 – 100 %) and good specificities (72 – 94 %) [1]. In the current study, CE-MRI at 3 T achieved similar results with excellent diagnostic accuracy

(93 %). With the use of a high-resolution MR imaging protocol at 3 T, no cancers were missed, but there were 12 FP lesions, which consisted of five NME lesions and seven mass lesions, and which exhibited suspicious morphological and/or kinetic features. These findings are in good agreement with previously reported data showing that there are limits to what is achievable with CE-MRI alone [2, 19, 30–32]. Several studies have demonstrated that, with the use of additional MR parameters, such as diffusion-weighted MR imaging or proton MR spectroscopy, an increase in diagnostic accuracy is achievable [2, 19]. However, in patients with certain contra-indications to MRI [12] who cannot benefit from multiparametric MRI, imaging modalities other than MRI would be of more value. The results of our study show that ^{18}F-FDG PET/CT may be such a modality in patients who are not candidates for MRI.

The current study had some limitations. The study included only a small number of patients with DCIS or invasive lobular carcinoma (ILC). Therefore, the findings regarding the performance of both ^{18}F-FDG PET/CT and CE-MRI in these subgroups should be regarded with caution. Nevertheless, the results in DCIS [33] and ILC [34] are in good agreement with previously published data. In addition, this was a prospective study enrolling consecutive patients with suspicious breast lesions, and therefore disease prevalence was high, and does not reflect the prevalence in a screening population. However, in this setting the distribution of malignant histopathological subtypes was as expected indicating that our patients were a representative patient population. Furthermore, the aim of the study was not to determine the indications for prone breast PET/CT, but merely to assess its diagnostic accuracy and the factors that influence accuracy. Further

studies are necessary to elucidate the potential application of prone breast PET/CT.

In conclusion, both ^{18}F-FDG PET/CT and CE-MRI at 3 T are useful in the assessment of breast tumours. Both imaging modalities achieve a high diagnostic accuracy. In breast lesions <10 mm, the diagnostic accuracy of both modalities deteriorates. In contrast to visual PET/CT assessment, SUV_{MAX} is not helpful in differentiating malignant from benign breast lesions. ^{18}F-FDG PET/CT can be considered an alternative imaging modality in patients who are not candidates for CE-MRI.

References

1. Sardanelli F, Boetes C, Borisch B, Decker T, Federico M, Gilbert FJ, et al. Magnetic resonance imaging of the breast: recommendations from the EUSOMA working group. Eur J Cancer. 2010;46:1296–316. doi:10.1016/j.ejca.2010.02.015.
2. Pinker K, Bogner W, Baltzer P, Gruber S, Bickel H, Brueck B, et al. Improved diagnostic accuracy with multiparametric magnetic resonance imaging of the breast using dynamic contrast-enhanced magnetic resonance imaging, diffusion-weighted imaging, and 3-dimensional proton magnetic resonance spectroscopic imaging. Invest Radiol. 2014;49:421–30. doi:10.1097/RLI.0000000000000029.
3. Pinker K, Bogner W, Baltzer P, Karanikas G, Magometschnigg H, Brader P, et al. Improved differentiation of benign and malignant breast tumors with multiparametric 18fluorodeoxyglucose positron emission tomography magnetic resonance imaging: a feasibility study. Clin Cancer Res. 2014;20:3540–9. doi:10.1158/1078-0432.CCR-13-2810.
4. Pinker K, Grabner G, Bogner W, Gruber S, Szomolanyi P, Trattnig S, et al. A combined high temporal and high spatial resolution 3 Tesla MR imaging protocol for the assessment of breast lesions: initial results. Invest Radiol. 2009;44:553–8. doi:10.1097/RLI.0b013e3181b4c127.
5. Kuhl CK, Jost P, Morakkabati N, Zivanovic O, Schild HH, Gieseke J. Contrast-enhanced MR imaging of the breast at 3.0 and 1.5 T in the same patients: initial experience. Radiology. 2006;239:666–76.
6. Butler RS, Chen C, Vashi R, Hooley RJ, Philpotts LE. 3.0 Tesla vs 1.5 Tesla breast magnetic resonance imaging in newly diagnosed breast cancer patients. World J Radiol. 2013;5:285–94. doi:10.4329/wjr.v5.i8.285.
7. Koolen BB, Vogel WV, Vrancken Peeters MJ, Loo CE, Rutgers EJ, Valdes Olmos RA. Molecular imaging in breast cancer: from whole-body PET/CT to dedicated breast PET. J Oncol. 2012;2012:438647. doi:10.1155/2012/438647.
8. Moy L, Noz ME, Maguire Jr GQ, Ponzo F, Deans AE, Murphy-Walcott AD, et al. Prone mammoPET acquisition improves the ability to fuse MRI and PET breast scans. Clin Nucl Med. 2007;32:194–8. doi:10.1097/01.rlu.0000255055.10177.80.
9. Yutani K, Tatsumi M, Uehara T, Nishimura T. Effect of patients' being prone during FDG PET for the diagnosis of breast cancer. AJR Am J Roentgenol. 1999;173:1337–9.
10. Avril N, Adler LP. F-18 fluorodeoxyglucose-positron emission tomography imaging for primary breast cancer and loco-regional staging. Radiol Clin N Am. 2007;45:645–57. doi:10.1016/j.rcl.2007.05.004.
11. Koolen BB, van der Leij F, Vogel WV, Rutgers EJ, Vrancken Peeters MJ, Elkhuizen PH, et al. Accuracy of 18F-FDG PET/CT for primary tumor visualization and staging in T1 breast cancer. Acta Oncol. 2014;53:50–7. doi:10.3109/0284186X.2013.783714.
12. Expert Panel on MR Safety, Kanal E, Barkovich AJ, Bell C, Borgstede JP, Bradley Jr WG, et al. ACR guidance document on MR safe practices: 2013. J Magn Reson Imaging. 2013;37:501–30. doi:10.1002/jmri.24011.
13. Knausl B, Hirtl A, Dobrozemsky G, Bergmann H, Kletter K, Dudczak R, et al. PET based volume segmentation with emphasis on the iterative TrueX algorithm. Z Med Phys. 2012;22:29–39. doi:10.1016/j.zemedi.2010.12.003.
14. Rapisarda E, Bettinardi V, Thielemans K, Gilardi MC. Image-based point spread function implementation in a fully 3D OSEM reconstruction algorithm for PET. Phys Med Biol. 2010;55:4131–51. doi:10.1088/0031-9155/55/14/012.
15. Kumar R, Chauhan A, Zhuang H, Chandra P, Schnall M, Alavi A. Clinicopathologic factors associated with false negative FDG-PET in primary breast cancer. Breast Cancer Res Treat. 2006;98:267–74. doi:10.1007/s10549-006-9159-2.
16. Kumar R, Chauhan A, Zhuang H, Chandra P, Schnall M, Alavi A. Standardized uptake values of normal breast tissue with 2-deoxy-2-[F-18]fluoro-D-glucose positron emission tomography: variations with age, breast density, and menopausal status. Mol Imaging Biol. 2006;8:355–62. doi:10.1007/s11307-006-0060-5.
17. Sickles EA, D'Orsi CJ. ACR BI-RADS® follow-up and outcome monitoring. In: D'Orsi CJ, Sickles EA, Mendelson EB, Morris EA, et al. ACR BI-RADS® atlas, breast imaging reporting and data system. Reston, VA: American College of Radiology; 2013.
18. Kuhl CK, Schild HH, Morakkabati N. Dynamic bilateral contrast-enhanced MR imaging of the breast: trade-off between spatial and temporal resolution. Radiology. 2005;236:789–800.
19. Pinker K, Bickel H, Helbich TH, Gruber S, Dubsky P, Pluschnig U, et al. Combined contrast-enhanced magnetic resonance and diffusion-weighted imaging reading adapted to the "Breast imaging reporting and data system" for multiparametric 3-T imaging of breast lesions. Eur Radiol. 2013;23:1791–802. doi:10.1007/s00330-013-2771-8.
20. Krishnamurthy S, Bevers T, Kuerer H, Yang WT. Multidisciplinary considerations in the management of high-risk breast lesions. AJR Am J Roentgenol. 2012;198:W132–40. doi:10.2214/AJR.11.7799.
21. Goerres GW, Michel SC, Fehr MK, Kaim AH, Steinert HC, Seifert B, et al. Follow-up of women with breast cancer: comparison between MRI and FDG PET. Eur Radiol. 2003;13:1635–44. doi:10.1007/s00330-002-1720-8.
22. Imbriaco M, Caprio MG, Limite G, Pace L, De Falco T, Capuano E, et al. Dual-time-point 18F-FDG PET/CT versus dynamic breast MRI of suspicious breast lesions. AJR Am J Roentgenol. 2008;191:1323–30. doi:10.2214/AJR.07.3439.
23. Caprio MG, Cangiano A, Imbriaco M, Soscia F, Di Martino G, Farina A, et al. Dual-time-point [18F]-FDG PET/CT in the diagnostic evaluation of suspicious breast lesions. Radiol Med. 2010;115:215–24. doi:10.1007/s11547-009-0491-6.

24. Heusner TA, Freudenberg LS, Kuehl H, Hauth EA, Veit-Haibach P, Forsting M, et al. Whole-body PET/CT-mammography for staging breast cancer: initial results. Br J Radiol. 2008;81:743–8. doi:10.1259/bjr/69647413.

25. Vidal-Sicart S, Aukema TS, Vogel WV, Hoefnagel CA, Valdes-Olmos RA. Added value of prone position technique for PET-TAC in breast cancer patients. Rev Esp Med Nucl. 2010;29:230–5. doi:10.1016/j.remn.2010.05.002.

26. Choi YJ, Shin YD, Kang YH, Lee MS, Lee MK, Cho BS, et al. The effects of preoperative (18)F-FDG PET/CT in breast cancer patients in comparison to the conventional imaging study. J Breast Cancer. 2012;15:441–8. doi:10.4048/jbc.2012.15.4.441.

27. Mavi A, Urhan M, Yu JQ, Zhuang H, Houseni M, Cermik TF, et al. Dual time point 18F-FDG PET imaging detects breast cancer with high sensitivity and correlates well with histologic subtypes. J Nucl Med. 2006;47:1440–6.

28. Eubank WB, Mankoff DA. Evolving role of positron emission tomography in breast cancer imaging. Semin Nucl Med. 2005;35:84–99. doi:10.1053/j.semnuclmed.2004.11.001.

29. Avril N, Propper D. Functional PET imaging in cancer drug development. Future Oncol. 2007;3:215–28. doi:10.2217/14796694.3.2.215.

30. Ei Khouli RH, Jacobs MA, Mezban SD, Huang P, Kamel IR, Macura KJ, et al. Diffusion-weighted imaging improves the diagnostic accuracy of conventional 3.0-T breast MR imaging. Radiology. 2010;256:64–73. doi:10.1148/radiol.10091367.

31. Partridge SC, DeMartini WB, Kurland BF, Eby PR, White SW, Lehman CD. Quantitative diffusion-weighted imaging as an adjunct to conventional breast MRI for improved positive predictive value. AJR Am J Roentgenol. 2009;193:1716–22. doi:10.2214/AJR.08.2139.

32. Baltzer PA, Benndorf M, Dietzel M, Gajda M, Runnebaum IB, Kaiser WA. False-positive findings at contrast-enhanced breast MRI: a BI-RADS descriptor study. AJR Am J Roentgenol. 2010;194:1658–63. doi:10.2214/AJR.09.3486.

33. Lehman CD. Magnetic resonance imaging in the evaluation of ductal carcinoma in situ. J Natl Cancer Inst Monogr. 2010;2010:150–1. doi:10.1093/jncimonographs/lgq030.

34. Mann RM, Loo CE, Wobbes T, Bult P, Barentsz JO, Gilhuijs KG, et al. The impact of preoperative breast MRI on the re-excision rate in invasive lobular carcinoma of the breast. Breast Cancer Res Treat. 2010;119:415–22. doi:10.1007/s10549-009-0616-6.